Original Article

Quality Comparison of Decellularized Omentum Prepared by Different Protocols for Tissue Engineering Applications

Khatereh Fazelian-Dehkordi, Ph.D.[1], Sayed Fakhroddin Mesbah Ardekani, Ph.D.[1], Tahereh Talaei-Khozani, Ph.D.[2, 3*]

1. Department of Anatomical Sciences, Shiraz University of Medical Sciences, Shiraz, Iran
2. Histomorphometry and Stereology Research Center, Shiraz University of Medical Sciences, Shiraz, Iran
3. Tissue Engineering Lab, Anatomy Department, Shiraz University of Medical Sciences, Shiraz, Iran

**Corresponding Address: P.O.Box: 7134845794, Histomorphometry and Stereology Research Center, Shiraz University of Medical Sciences, Shiraz, Iran*
Email: talaeit@sums.ac.ir

Received: 07/February/2021, Accepted: 18/July/2021

Abstract

Objective: Decellularized greater omentum (GOM) is a good extracellular matrix (ECM) source for regenerative medicine applications. The aim of the current study was to compare the efficiency of three protocols for sheep GOM decellularization based on sufficient DNA depletion and ECM content retention for tissue engineering application.

Materials and Methods: In this experimental study, in the first protocol, low concentrations of sodium dodecyl sulfate (SDS 1%), hexane, acetone, ethylenediaminetetraacetic acid (EDTA), and ethanol were used. In the second one, a high concentration of SDS (4%) and ethanol, and in the last one sodium lauryl ether sulfate (SLES 1%) were used to decellularize the GOM. To evaluate the quality of scaffold prepared with various protocols, histochemical staining, DNA, and glycosaminoglycan (GAGs) quantification, scanning electron microscopy (SEM), Raman confocal microscopy, Bradford assay, and ELISA were performed.

Results: A comparison of DNA content showed that SDS-based protocols omitted DNA more efficiently than the SLES-based protocol. Histochemical staining showed that all protocols preserved the neutral carbohydrates, collagen, and elastic fibers; however, the SLES-based protocol removed the lipid droplets better than the SDS-based protocols. Although SEM images showed that all protocols preserved the ECM architecture, Raman microscopy, GAGs quantification, total protein, and vascular endothelial growth factor (VEGF) assessments revealed that SDS 1% preserved ECM more efficiently than the others.

Conclusion: The SDS 1% can be considered a superior protocol for decellularizing GOM in tissue engineering applications.

***Keywords**:* Decellularization, Extracellular Matrix, Greater Omentum, Scaffold, Tissue Engineering

Cell Journal(Yakhteh), Vol 24, No 5, May 2022, Pages: 267-276

Citation: **Fazelian-Dehkordi Kh, Mesbah Ardekani SF, Talaei-Khozani T. Quality comparison of decellularized omentum prepared by different protocols for tissue engineering applications. Cell J. 2022; 24(5): 267-276. doi: 10.22074/cellj.2022.7968.**

Introduction

Native autologous greater omentum (GOM) has been used as a flap in reconstructive surgery in many organs such as the esophagus, trachea, duodenum small intestine, and bladder. Native GOM has rich vascularity, high angiogenic activity, innate immune function, the capability to adhere to the surrounding structures, and high production sufficiency of growth factors (1). Omentum induces neovascularization; is involved in hemostasis, tissue healing, and regeneration; and acts as an *in vivo* incubator for culturing the cells and tissues (2). These properties make it a boon for regenerative medicine applications (3). As the GOM is used in many surgical reconstructions, transplantation of decellularized GOM decreases the chance of graft rejection (4).

Decellularized GOM has several applications in regenerative medicine. Autologous decellularized omentum provided appropriate structural and mechanical supports for the cardiac cells to generate contraction *in vitro* (5). Porcine decellularized GOM has been reported to support *in vitro* cell adhesion and growth (3). The metabolic rescue has been previously reported for human diabetic adipose-derived mesenchymal stem cells after culturing on decellularized GOM. The report indicates that the extracellular matrix (ECM) of the omentum has specific components with the capability to regulate cell functions. ECM of the omentum regulates adipocyte differentiation, glucose uptake, and lipolysis (6). Being decellularized with well-preserved architecture, including vessel framework, makes it a better choice for reconstructive surgery or tissue engineering. Due to the collagen and glycosaminoglycan (GAGs) content (3), decellularized tissues such as GOM can be gelatinized and form hydrogel for cell encapsulation (7). Recently, GOM-based 3D decellularized matrix has been used to fabricate the engineered cardiac tissue (8). Decellularized GOM has been used to prepare a hydrogel for cardiac cell encapsulation (5). Also, decellularized omentum was used as a platform for culturing the cells isolated from the human kidney,

urothelial cells, and endothelial cells (9).

The ECM, as an essential part of each tissue, has many bioactive macromolecules such as glycoproteins, GAGs, various growth factors, and cytokines. Natural scaffolds from decellularized tissues provide a biomimicry framework to protect cell adhesion, proliferation, migration, and functions; some of these decellularized scaffolds have been successfully transplanted in both animal models (10) and human clinical trials (11).

The target of the decellularization methods is to diminish any detrimental impact of decellularizing agents on the constitution and biological activity of the residual ECM along with cellular and nuclear material depletion. In the most common decellularization protocols, a combination of chemical, enzymatic, and physical approaches is used (11). These protocols are usually started with the cell membrane disruption using different physical treatments or ionic detergents, followed by washing the cellular debris with enzymes and detergents to solubilize and finally remove the cellular debris from the ECM (12). The freeze-thaw cycling is a useful method for disrupting the cell membranes (3); however, its administration alone cannot lead to the proper removal of all the nuclear material from the tissue (13). Therefore, its combination with other methods is used to remove cellular components more efficiently. Non-enzymatic agents such as ethylenediaminetetraacetic acid (EDTA) disrupt cell adhesion by chelating divalent cations such as Ca^{2+} and Mg^{2+}. These divalent ions are involved in attachment of cells to collagen and fibronectin (12). Also, treating the tissues with hyperosmolar and hypo-osmolar solutions (14) leads to cell lysis and disruption of DNA-proteins interaction (15). Ethanol and glycerol act as dehydrators in decellularization protocols and contribute to tissue dehydration and cell lysis. Acetone removes lipids from decellularized tissues (16).

The most popular protocols for GOM decellularization are based on the protocols used for adipose tissue decellularization (3). In the current study, we checked the mechanical, enzymatic, and lipid extractive mechanisms in the quality of cell lysis, DNA, GAGs, total protein, and vascular endothelial growth factor (VEGF) content to develop a proper scaffold for reconstructive surgery. Therefore, aims of this study was to evaluate the efficacy of three different protocols for GOM decellularization and compare the DNA depletion and ECM and ultra-structure retention for regenerative medicine application.

Materials and Methods

Experimental design

This experimental study was approved by the Ethics Committee of Shiraz University of Medical Sciences (IR.SUMS.REC.1396.S1013). The fresh GOM of healthy sheep was obtained from the city slaughterhouse. The tissues were washed with phosphate-buffered saline (PBS); after that, they were cut into small pieces (2×2 cm). Each piece (n=10-15) was treated with a specific decellularization protocol, as described in the following section. After lyophilizing the decellularized GOM, they were sterilized with UV light (wavelength: 253.7 nm) for 30 minutes. Finally, each piece (10 mg) was digested with 10 mg of pepsin [Biochemical (BDH), England] and 20 mL of 0.1 M Hydrochloric acid (HCL, pH=1.6-2.5) for 48-72 hours. All steps of the procedures were carried out at room temperature on an orbital shaker. Also, penicillin (100 IU/ml, Gibco, USA) and streptomycin (100 µg/Ml, Gibco, USA) were used to minimize microbial contamination.

Protocol-1 (sodium dodecyl sulfate [SDS 1%]): was based on the work done by Soffer-Tsur et al. (4) with some modifications. The osmotic shock was applied to fresh pieces of GOM by incubating in a hypotonic buffer containing 10 mM Tris and 5 mM EDTA for 24 hours (with three changes), followed by dehydrating in 70% and 100% ethanol for 30 minutes for each step. Then, lipid extraction was performed by incubation in 100% acetone for 24 hours (with three changes). Rehydration was performed by incubation the tissue pieces in 100% ethanol for 30 minutes, followed by overnight incubation in 70% ethanol at 4°C. After washing with PBS at pH=7.4, the samples were incubated again in the hypotonic solution for 2 hours. Further cell lysis was achieved by treating the pieces in 1% SDS dissolved in PBS for 24 hours (with 2 changes). Another hypotonic shock was done for 2 hours, and the samples were incubated again in 1% SDS and then in 2.5 mM sodium deoxycholate for the same period. The trace of detergents was washed by PBS and then by 50 mM Tris containing 1 mM $MgCl_2$ at pH 8.0 for 1 hour. Further lipid extraction and dehydration were performed with 70% and 100% ethanol for 30 minutes, followed by treating the samples in 100% acetone for 30 minutes (3 changes). Finally, 3-changes of hexane: acetone [60/40 (v/v)] for 24 hours were used to extract the polar lipid. The defatted tissues were rehydrated by treating the samples with decreasing ethanol concentration (100 and 70%) for 30 minutes at 4°C, followed by washing in PBS and double distilled water three times each. The decellularized tissue was frozen (-20°C) overnight and lyophilized by a freeze dryer (CHIRST, Alpha 1-2 LD plus, Germany, -50°C).

Protocol-2 (SDS 4%): freeze-thaw cycles (n=3) and mechanical rubbing of the pieces of GOM underwater were achieved for an hour. Subsequently, the samples were soaked in distilled water containing Penicillin (100 IU/mL, Gibco, USA) and Streptomycin (100 µg/mL, Gibco, USA) for 48 hours on a stirrer. After that, they were incubated in SDS 4% for 3 days under agitation using a stirrer and then rinsed in PBS. Rehydration and lipid extraction were done in the same way as performed for protocol-1. After washing with PBS and dehydrating

in 70% and 100% ethanol for 30 minutes, the samples were incubated in 2% SDS for 1 day. After another washing with PBS and distilled water, the pieces were finally lyophilized.

Protocol-3 [sodium lauryl ether sulfate (SLES 1%)]: freeze-thaw cycles and the mechanical rubbing were performed in the same condition as in SDS 4%. The GOM was cut into pieces and incubated in Sodium lauryl ether sulfate 1% (SLES, Kimia Sanaat Ataman Co. Tehran, Iran) for 72 hours at 18-20°C on a magnetic stirrer (with three changes). Subsequently, they were washed with PBS three times to remove the cell remnants and trace of chemical reagents. The decellularized tissue was frozen (-20°C) and lyophilized (17).

Decellularization efficiency

Pieces from intact and decellularized sheep omenta were fixed in formalin and prepared for paraffin-embedded histological sectioning. The samples were sectioned at a thickness of 5 µm and mounted on glass slides. The slides were stained with 0.1% Hoechst (33342, Sigma-Aldrich, USA) in PBS and H&E (Merck, Geneva, Switzerland) to assess the nuclear component removal.

DNA content analysis

DNA content of the intact and decellularized omenta (n=3) was assessed using dsDNA Assay Kit (Qiagen, Germany), according to the manufacturer's Guideline. Briefly, the lyophilized samples were cut into pieces. 25 mg of GOM was weighted and digested with proteinase K at 56°C. After washing, 200 µL of 96% ethanol was used to extract DNA; then, the pieces were transferred to DNeasy Mini spin column to elute DNA. The ratio of DNA to protein was assessed by a spectrophotometer (Nano drop Technologies Inc, Wilmington, USA) at 260/280 nm.

Retention of extracellular matrix content

Masson's Trichorom and aldehyde fuchsine staining were done to assess collagen and elastic fiber content preservation in intact and decellularized GOM. Images were acquired using standard bright field techniques (Olympus Japan).

To evaluate the retention of acidic GAGs and neutral carbohydrates, we stained the intact and decellularized tissues with Alcian blue and methylene blue (Sigma-Aldrich, USA) at pH=1 and Periodic acid–Schiff, respectively. Lipid removal was verified by staining the 5-µm frozen sections of intact and decellularized tissues with Oil Red-O Stain (Sigma-Aldrich, USA).

Quantification of glycosaminoglycan content

To determine the GAGs content of the intact and decellularized GOM, we performed a modified protocol prepared by Geerts et al. (18). About 100 mg of the lyophilized decellularized GOM was hydrolyzed using 0.25 mL of 6 M HCL (Fisher, Waltham, MA) for 20 hours at 95°C. After that, the samples were allowed to cool at room temperature. Subsequently, 250 mL methylene blue was added to 10 mL of the sample, and the optical absorbance was immediately evaluated at a wavelength of 510 nm. To measure the amount of GAG content, the optical density of the samples was compared with a calibration curve obtained by serial dilution of heparin in PBS.

Scanning electron microscopy

To evaluate the ultra-architecture of the decellularized GOM, we performed scanning electron microscopy (SEM). One part of each decellularized GOM was fixed with 2.5% glutaraldehyde (Sigma-Aldrich, St. Louis, MO, USA) in 0.2M PBS at pH=7.4 for 2 hours at 4°C. Subsequently, they were dehydrated in an increasing graded series of ethanol (50-100%). Finally, the samples were dried at the critical point and coated with gold by Q150R- ES sputter coater (QuorumTechnologies, UK); then, they were observed, and photography was taken by a VEGA3 microscope (TESCAN, Czech Republic).

Confocal Raman microscopy assessment

The Raman spectra of the GOM decellularized by three protocols and intact pieces were recorded. The laser power level was 50 mW using the excitation laser wavelength of 785 nm. In the current study, the samples were analyzed using Raman spectra in the range of 500 to 2000 cm^{-1} with a resolution of 4 cm^{-1}.

Quantitative Measurement of VEGF with sandwich-ELISA

The content of VEGF in the decellularized tissues was measured using Enzyme-Linked Immunosorbent Assay kit (ELISA, bioassay technology laboratory). The plate was pre-coated with sheep VEGF antibody. Forty µl pepsin-treated decellularized GOMs, and 10 µl anti-VEGF antibody were added to the sample wells. Moreover, 50 µl streptavidin-HRP was added to the sample and standard wells. Subsequently the wells were mixed and incubated for 60 minutes at 37°C. After washing the unbound Streptavidin-HRP, substrate solution was added to develop color. The reaction was terminated by adding an acidic stop solution, and the absorbance was measured at 450 nm. The amount of VEGF was also calibrated and normalized.

Protein assessment

The Bradford assay determined the total protein concentration of each decellularized sample and compared it with that intact GOM. Protein concentration measurement relies on the dye molecule, Coomassie brilliant blue G-250 (Fisher Scientific, USA), binding to basic amino acids such as lysine. The samples were digested using 0.25% pepsin in HCL (0.1 M) at a dilution

of 1:10 (gram of the pieces of GOM: pepsin). Subsequently, the protein content was measured by adding 50µL of each sample and a serial dilution of BSA, as standards, to 200 µL Bradford reagent in a 96 well micro-plate. Absorbance at 595 nm was recorded after 5 minutes by ELISA reader (Thermo Scientific Varioskan Flash Multimode Reader) (19).

MTT test on fibroblast cells

To evaluate the toxicity, we exposed the human fibroblast cells isolated from the gingiva at a density of 2×10^4 to decellularized GOM prepared with all three methods at concentrations of 0.5, 0.25, 0.125, and 0.625 mg/mL; the results were compared with the cells cultured in the absence of decellularized GOM as the control culture. Decellularized GOM was dissolved in Dulbecco's Modified Eagle Medium (DMEM, Gibco, USA) containing 15% fetal bovine ferum (FBS, Gibco Paisley, USA), 2 mL L-Glutamine 1%, 100 IU/mL penicillin, and 100 µg/mL Streptomycin. Cell viability was assessed by MTT method after 1, 3, and 7 days with 3 replications for each concentration. The supernatant was discarded, and MTT (1 mg/mL) was added to all wells and incubated for 3-4 hours. Then, Dimethyl sulfoxide (300 µL) (Sigma-Aldrich, USA) was added to the wells to dissolve the formazan crystals for 15 minutes. Finally, the optical density (OD) was evaluated at 595 nm with a spectrophotometer (Nanodrop Technologies Inc, Wilmington, USA).

Statistical analysis

The data were presented as mean ± standard error (SE). One-way ANOVA and the Tukey post hoc tests were used to compare the mean values. All analyses were performed using Graph Pad Prism version 6.00 For Windows (Graphpad, USA). A $P<0.0001$ was considered significant.

Results

Gross observation of the decellularized GOM revealed lipid loss, color change from yellow to colorless, and an increase in transparency. Although a slight decrease in consistency was detected, the shape of the decellularized pieces, vascular architecture, and homogeneity were preserved. There was no deformation or disintegration regardless of the protocol used for decellularization (Fig.1A-F).

Scanning electron microscopy microscopy

Scanning electron microscopy (SEM) evaluation confirmed the ultra-architecture integrity and efficiency of cell depletion after various decellularization processes. Lower magnification photomicrographs of decellularized GOM showed fibers that formed porous structures. The ultra-architecture of the decellularized GOM was similar in all pieces of GOM treated with different protocols (Fig.1G-I).

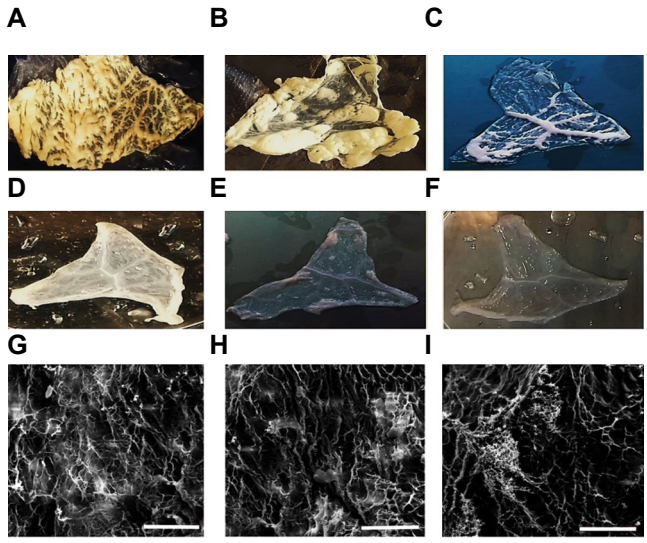

Fig.1: The gross morphology of the omentum in different decellularization phase and SEM images of the omentum decellularized by varous protocoles. **A-F.** As a result of lipid loss, the color of the GOM samples changed from yellow (undecellularized omentum) to colorless (decellularized omentum). SEM assessment showed ultra-architecture of the decellularized tissues was devoid of cells after decellularization by G. SDS 1%, H. SDS 4% and I. SLES 1% protocols (scale bar: 100 µm). SEM; Scanning electron microscope, GOM; Greater omentum, SDS; Sodium dodecyl sulfate, and SLES; Sodium lauryl ether sulfate.

Cell removal efficacy

Hoechst and H&E staining revealed that all protocols could remove the cells to an acceptable value because no cell nucleus was observed. The histological sections also showed some degree of morphological modifications of the processed tissues compared to native ones. In all decellularized tissues, fat extraction with polar and nonpolar solvents led to the absence of lipids and adipocytes; as a result, the honeycomb morphology, which can be observed in naïve tissue, was destroyed some extent. Accordingly, H&E staining revealed the presence of a few nuclei in the tissues processed by SLES 1%. Morphological comparison of the tissues prepared by various protocols revealed that all protocols showed a degree of destructive impact on ECM (Fig.2).

In all protocols, decellularization led to a significant decrease in the DNA content compared to intact GOM. Although a trace of DNA remained in all decellularized GOM, the amount of DNA was less than 50 ng/mg (standard rate). This amount is not enough to cause an immunological reaction after transplantation (20). A comparison of different protocols showed that DNA content was significantly less in the GOM prepared with SDS 1 and 4% than that prepared with SLES 1% ($P=0.05$, Fig.2A).

Glycosaminoglycan retention

Although Alcian blue and methylene blue staining

showed some extent of GAG retention in the omenta prepared with all protocols, quantification revealed a significant reduction in GAGs content in the decellularized omenta compared to the intact one (Fig.2). The best protocol for GAG retention was SDS 1%, while the amount of GAGs was significantly higher than the samples decellularized with the other two protocols. Overall, the SDS-based detergents showed a low degree of destruction for GAGs than SLES (Fig.2B).

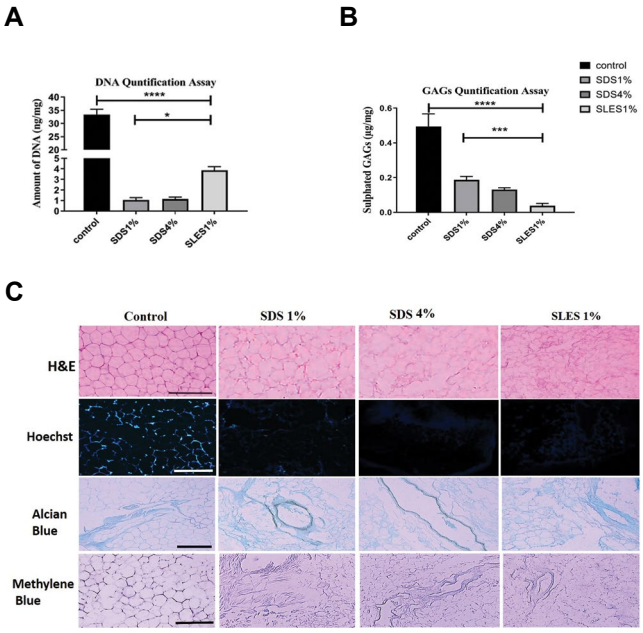

Fig.2: The graphs show the comparison of the DNA and GAGs quantification in different groups and micrographs show the decellularized GOM that stained by H&E, Hoechst, Acian blue and Methylen blue. **A.** The graph compares DNA quantification after decellularization with different methods and control**.** Data are expressed as the mean ± standard error of the mean (SEM), n=3 per group. ****; Indicates the significant difference with the control group (undecellularized tissue), (P<0.0001), *; Indicates the significant difference with SDS 1%, (P=0.044). **B.** The graph compares GAGs content of decellularized GOM with control. Graph showed that SDS 1% preserved the GAG content better than the other protocols. n=3 per group, ****; Indicates the significant difference with the control group, (P<0.0001), ***; Indicates the significant difference with using SDS 1%, (P=0.0061), **C**. Micrographs show H&E, Hoechst, Acian blue and Methylen blue staining of decellularized GOM (scale bar: 100 µm). GAGs; Glycosaminoglycans, GOM; Greater omentum, H&E; Hematoxylin and eosin, and SDS, Sodium dodecyl sulfate.

Retention of extracellular matrix contents

In all protocols, histochemical staining showed retention of ECM components after decellularization. Accordingly, periodic acid-schiff (PAS) staining showed the persistence of neutral carbohydrates. Masson's Trichrome and aldehyde fuchsine staining also demonstrated the retention of collagen and elastic fibers, respectively. All decellularization protocols showed an acceptable lipid removal, as indicated by Oil Red staining; however, lipid droplets were extracted more efficiently in SLES-treated scaffolds (SLES 1%). More similarity of the matrix structure in SLES-treated samples with native tissue, and sufficient fat removal, support the claim that a nonpolar solvent alone is more appropriate for fat removal (Fig.3).

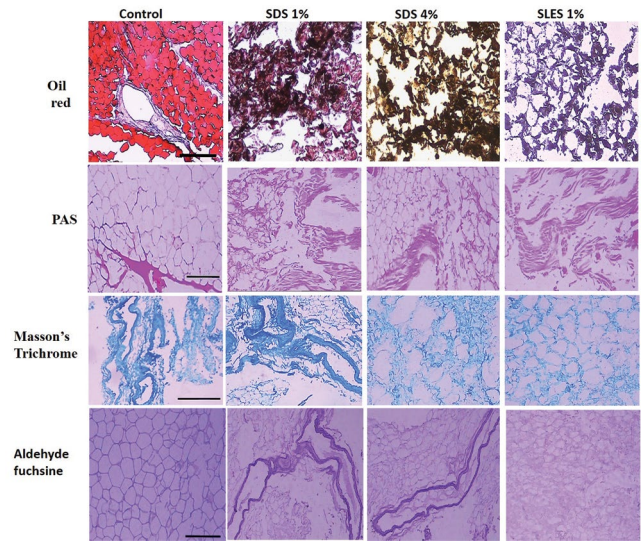

Fig.3: Histochemical assessments of decellularized omenta obtained by SDS 1%, SDS 4% and SLES 1% and undecellularized tissue (control) (scale bar: 100 µm). SDS; Sodium dodecyl sulfate and SLES; Sodium lauryl ether sulfate.

Bradford assay

Although the protein content of decellularized scaffolds was significantly washed out by the decellularization process regardless of the protocol (P<0.0001 for all), SDS 1% preserved the protein content significantly and more efficiently than the others (both P<0.0001). SLES showed a detrimental impact on the protein content so the pics of GOM treated with SLES 1% contained the least amount of protein compared to SDS-based protocols (P=0.0001, Fig.4A).

Quantitative measurement of VEGF concentration

VEGF, as the most abundant growth factor in the ECM of GOM, should be preserved after decellularization. To evaluate the preservation of this growth factor, we measured the level of VEGF as an example of growth factor content. Although VEGF was significantly washed in GOM treated by all protocols compared with the intact ones (control versus SDS 1% (P=0.0029), SDS 4% (P=0.0016), and SLES 1% (P=0.0003), VEGF was better preserved in the GOM prepared by SDS-based protocols compared to SLES-based ones (SDS 1% versus SLES 1%, P=0.0059) and SDS 4% versus SLES 1% (P=0.0139). VEGF washing off was significantly higher in the GOM prepared by SLES 1% (Fig.4B).

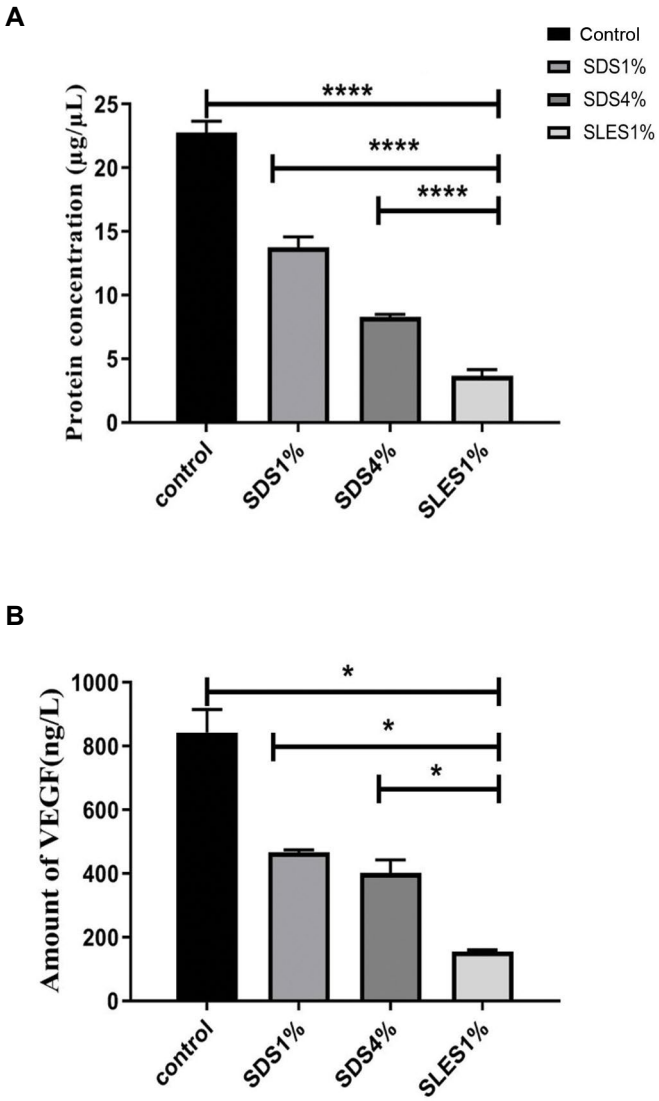

Fig.4: The graphs showed the protein and VEGF concentrations. **A.** Bradford assay showed a significant protein wash out after decellularization. Results are presented as mean µg protein per mg dry mass (n=3 per group), ****; Indicates the significant difference with the control group (P<0.0001), the omenta prepared by SDS 1% (P<0.0001), and SDS 4% (P=0.0001). **B.** ELISA assessment showed a significant decrease in the VEGF content after decellularization. Results are presented as the mean of VEGF (ng) per Liter dry mass (n=3 per group), *; Indicates the significant difference with the control group (P<0.05), SDS 1%, (P<0.05), and SDS 4%, (P<0.05). VEGF; Vascular endothelial growth factor , SDS; Sodium dodecyl sulfate, and ELISA; Enzyme-linked immunosorbent assay.

Raman spectrum

After normalization and baseline correction, both intact and decellularized omenta showed nearly similar Raman spectra. Peaks at 546 cm^{-1} and 607 cm^{-1} were assigned for Cholesterol. A peak at 1079 cm^{-1} signifies the triglycerides (fatty acids), and at 1100 cm^{-1} and 1129 cm^{-1} signifies the lipid. Bands at 862 cm^{-1} display phosphate groups, and the peak at 875 cm^{-1} expresses the stretch vibration of choline group N (CH 3)3, characteristic of phospholipids, phosphatidylcholine, and sphingomyelin. Bands at 1368 cm^{-1}, 1440 cm^{-1}, 1729, and 1742 cm^{-1} indicate phospholipids, lipid, and Ester group, respectively (21). Vibration at 1765 cm^{-1} for C = O stretch represents the lipid fraction. The intensity of all these bands decreased to a great extent in decellularized tissues, which indicated the successful lipid depletion by all protocols.

Bands assigned for protein were detected as well. Specific bands for amide I at 1655, 1667, and 1673 cm^{-1} and stretching vibration at 1544 cm^{-1} for Amide II was observed. Vibrations at 1250, 1253, 1267, and 1321 cm^{-1} determined amide III and peaks at 890 cm^{-1} and 963 cm^{-1} belong to protein content. A peak at 920 cm^{-1} assigned the C-C stretch of proline ring/glucose/lactic acid, and 938 cm-1 assigned the C-C stretch backbone (lipid and protein) (21).

The resonance at 818 cm^{-1} can be assigned for C-C stretching (collagen assignment). In addition, bands at 1004, 1036, 1067, 1451, 1587, and 1205 cm^{-1} represent phenylalanine presents in the collagen. Peaks for tryptophan and cytosine and guanine that indicate the presence of DNA can be found at 573, 1165, 1175, 1297 and 1548 cm^{-1}. Vibration at 940 cm^{-1} can be represented for carbohydrates as well. A peak at 1347 cm^{-1} represents an unknown mode. 1392 cm^{-1} C-N stretching represents the quinoid ring-benzoid ring-quinoid ring. Comparison of Raman spectra of intact and decellularized GOM revealed an impressive reduction in protein, collagen, and DNA content (22) (Fig.5).

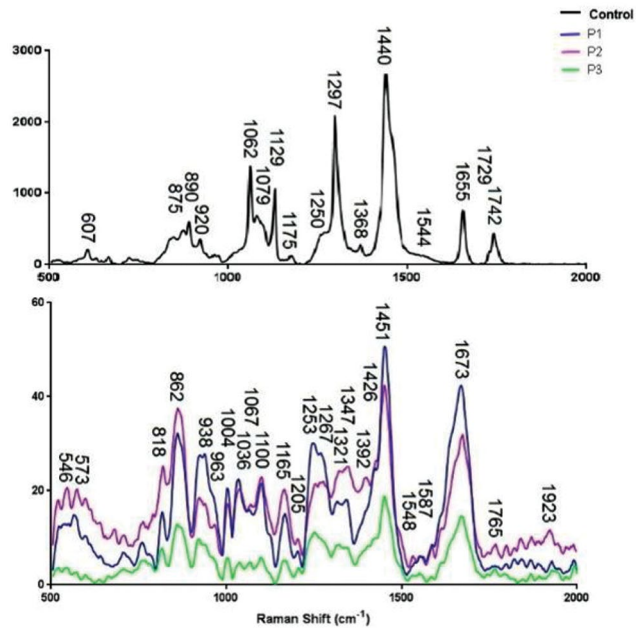

Fig.5: Raman spectra of native and decellularized omenta treatment using different decellularization protocols.

We also compared the intensity of the Raman spectra from the GOM prepared by various methods. Based on the Raman spectrum, SLES detergent decreased the amount

of lipid assigned at 862 and 1100 cm^{-1} compared to SDS detergent. A comparison of the intensity of the bands assigned for proteins at 1253 and 1267 cm^{-1} showed that the SDS 1% and SDS 4% better preserved these components than SLES 1%, a comparison of the band's intensity at 818 cm^{-1} also revealed better preservation of collagen by the SDS 4%. Besides, the Raman spectra showed that both SDS-based protocols retained collagen better than the SLES-based protocol. GAGs content was demonstrated in all decellularized scaffolds as indicated by vibration at 1062 cm^{-1}. Both SDS-based protocols preserved GAGs in the decellularized omenta better than the SLES-based protocols, and this finding confirmed the data obtained from the GAGs quantification assay. Furthermore, comparing the Raman spectra of commercially prepared SDS with SDS-treated samples revealed that SDS was completely washed out.

Overall, a comparison of various protocols showed that decellularization using SDS 1%, in combination with the other decellularization agents including EDTA, acetone-hexane, and ethanol, preserved collagen and protein better than the SLES-based protocol. Furthermore, administration of the higher SDS concentration in the SDS 4% extracted the lipid content more efficiently than SDS 1%, which used less amount of SDS (Fig.5).

Cytotoxicity of greater omentum

Cell viability was similar in all groups on the first day, regardless of the procedure. As the time progressed, the cell number increased in all conditions up to day 3; however, the cell viability remained constant up to day 7. In both SDS-treated cultures, the cell viability and proliferation significantly increased in the cultures exposed to 0.5% decellularized GOM compared to all the cultures exposed to lower concentrations as well as the control culture on day 3 (SDS 1% P=0.0001, P<0.0001 and SDS 4% P=0.0275, P<0.0001, P=0.0328). On day 7, cell viability was also significantly higher than all other groups in the cultures treated with 1% decellularized GOM treated groups (P=0.0454, P<0.0001, and P=0.0012). In the cultures treated with SDS 4%, a significant increase in cell viability was revealed in 0.5% decellularized GOM compared to 0.625% (P=0.0006).

In SLES-treated cultures, all concentrations of decellularized GOM had the same impact on the cell viability. However, cultures received 0.5% SLES, showed non-significant higher cell viability compared to all other groups on all days. Therefore, the data of this study showed that the influence of decellularized GOM on cell viability was depended on the type of detergent; however, SLES was not toxic for the cells as the cell viability in the cultures exposed to SLES-treated GOM was similar to the control culture (Fig.6).

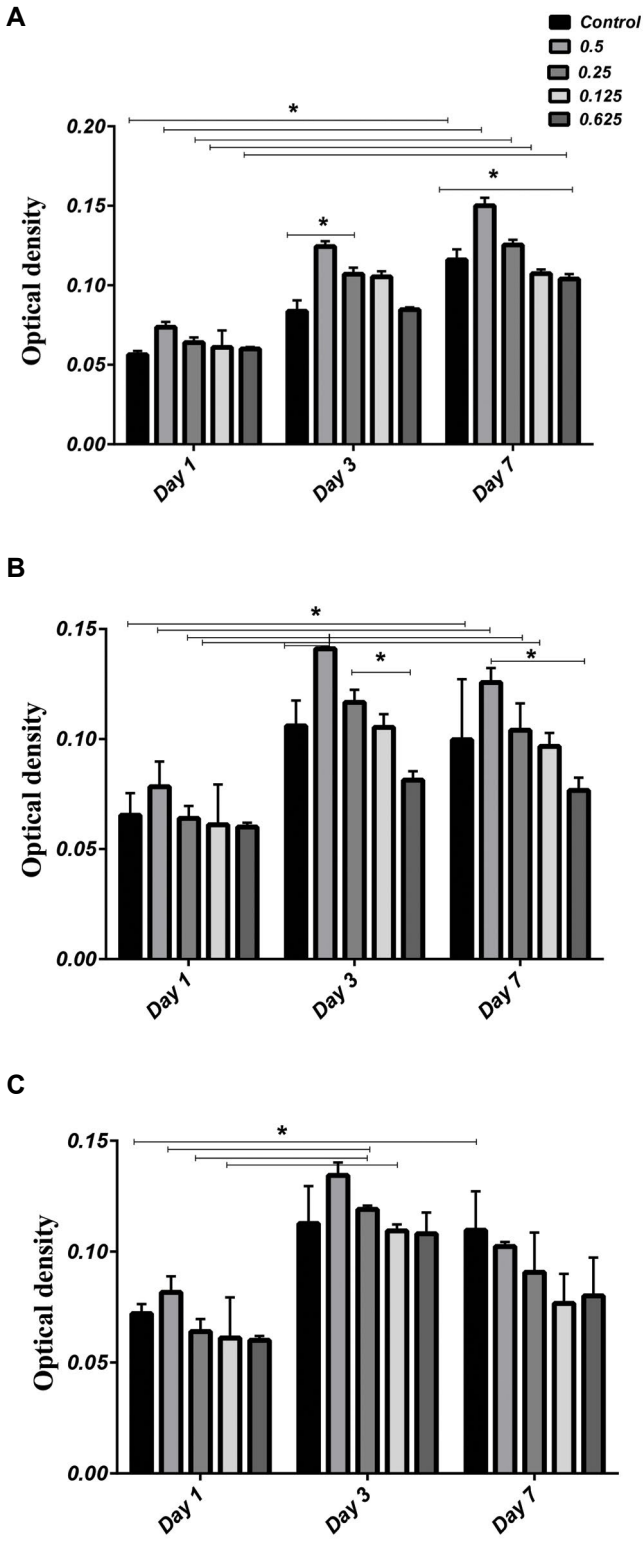

Fig.6: MTT test. Comparison of cell viability in the presence of different concentrations of decellularized GOM prepared with **A.** SDS 1%, **B.** SDS 4% and **C.** SLES (P<0.05).

Discussion

In the present research, we compared three protocols for decellularization of sheep GOM based on criteria such as damage to ECM constitutions, and ultra-architecture and efficient removal of cell and nuclear debris and lipid

extraction. Decellularization should ensure cellular and nuclear depletion and retain the ultra-architecture and composition of the ECM (20).

The data revealed that all protocols could remove DNA from the scaffolds to a great extent. The presence of DNA in the decellularized scaffolds can trigger inflammation; as a result, it can interfere with tissue repair (23). Regardless of the protocol, the DNA quantification assay revealed that the decellularized GOM contained less than 50 ng/mg dry weight (9), which has been reported as a safe DNA content that does not arouse inflammation after decellularized scaffold transplantation. However, previous works revealed mild inflammation after decellularized scaffold transplantation with the DNA content less than the allowed limit (24). Therefore, the recommended protocol is that which can minimize DNA remnant after decellularization. Our data showed that both SDS-containing protocols (SDS 1%, SDS 4%) significantly reduced the DNA content compared to the SLES-containing protocol (SLES 1%). Therefore, the decellularization method using SDS is better than SLES.

Besides DNA and cell debris removal, an appropriate decellularization protocol should retain the architecture and chemical structure of the ECM. H&E, aldehyde fuchsine, and Masson's Trichrome staining revealed that SDS and SLES-based protocols could preserve the tissue architecture. SEM images also confirmed ultra-architecture preservation after treatment with all protocols. SLES is a mild detergent (25) and has been previously used to decellularize organs such as the ovary (17), liver, and lung (25). The vascular architecture has been reported to be well preserved in SLES-treated scaffolds (26). Our Raman confocal microscopy and oil red staining confirmed that the best protocol for lipid extraction was the SLES-treated protocol; however, our data also indicated that SLES could wash out the protein, growth factors, and GAG content as well. Therefore, there should be a balance between the cell removal and ECM content retention for each recommended protocol.

GAGs, as the major components of the ECM, have numerous biological activities; they are involved in cell adhesion, cell growth regulation, and cell proliferation (27); therefore, the retention of GAGs can support the cell growth after recellularization of decellularized GOM. Our data showed that fat removal with SDS and hexane-acetone followed by mild detergents and hypertonic treatments had a less detrimental impact on the GAGs content than SLES. Sulfated GAGs carry negative charges, which stimulate the electrostatic interactions with growth factors and cytokines in ECM. Therefore, GAGs have roles in sequestration and controlled release of these factors into the cellular microenvironment.

Both SDS and SLES have detrimental impacts on protein and VEGF content; however, we showed that VEGF was better preserved in SDS-containing protocols. Previous studies have shown that SDS detergent disrupts the tissue ultrastructure (28) and growth factor deletion (29). On the other hand, SLES treatment has been shown to change the protein configuration (30); as a result, the antibodies cannot detect them properly in ELISA. Changes in the chemical configuration of proteins such as VEGF by SLES may also interfere with their functions. Better preservation of protein and VEGF by SDS-treated protocols may be due to the higher capability of SDS to preserve GAGs; as a result, the preserved GAGs may sequestrate the VEGF. Besides, some carbohydrates have been recommended to mitigate the cytotoxicity of biomaterial (31). The protocols retaining GAGs content may also help reduce the cytotoxicity of the trace of detergents used for decellularization. Therefore, GAGs retention within the ECM may be useful for engineering complex tissues (13). Confocal Raman spectroscopy can be considered a semi-quantitative method to characterize the biomolecular composition of native and decellularized tissues (32). Raman confocal microscopy confirmed extensive washout of GAGs by SLES-based protocol in our study.

In the current study, two SDS concentrations were used to show the optimal concentration of this detergent. SDS should remove the cells, and at the same time, it should retain the ECM content, including proteins such as VEGF. Our result showed higher concentration of SDS led to protein and VEGF washing. Along with our data, a study revealed that an increase in SDS concentration had harsh impacts on the matrix content of the decellularized kidney (33). In another study, two different SDS concentrations were used to decellularize ECM produced by the fibroblast sheet. It was found that a higher concentration of SDS increased the DNA depletion efficiency, although it accelerated the washing of the matrix and reduced mechanical properties of the decellularized sheet as well (23).

As GOM contains a large number of adipocytes, most of the protocols for GOM decellularization are based on the procedures for decellularization of the adipose tissue (32). Decellularization of GOM and adipose tissue has been obtained through some protocols which use cell rupture by mechanical procedures, solvent extraction, and enzymatic digestion (3, 6, 34). The protocols used in the current study provide a complex cell-free scaffold made up of a three-dimensional network of ECM, decellularized vascular bed, and preserved collagen and elastic fiber structure. A comparison of various protocols revealed that SDS-based protocols preserved GAGs and essential amino acids (phenylalanine, and hydroxyl proline) in the collagen structure better than SLES. However, SLES is a superior choice for lipid extraction. Previous studies on SDS have shown that long-term treatment with SDS has significant destructive effects on the natural ultrastructure of the ECM of the tissue and reduces GAGs and cytokines and has cytotoxic effects (35). However, the results of our study showed that the SDS detergent led to the preservation of the contents and structure of the ECM of grater omentum tissue. Based on the MTT test, SDS-based methods had a better impact on

the growth and survival of human gingival fibroblast cells without toxic effects than the SLES method.

GOM has often been used for angiogenic and regenerative properties (2). For instance, it has been used to coat the engineered colon, rectum, esophagus (36), stomach, and trachea. GOM has been used in osteochondral graft (37). Furthermore, autologous GOM has been used to treat perforated gastric/duodenal ulcers and decrease bleeding after hepatectomy or pancreaticoduodenectomy (38). Using allogeneic GOM that is more appropriate for standardizing the procedures and commercialization may arouse immunorejection. In decellularized GOM, the vascular architecture was preserved, and it might facilitate angiogenesis to the flaps (39). In this regard, SDS 1% is a superior choice as it can preserve VEGF better than other protocols. As decellularized GOM does not lead to inflammation, it could be taken from both living and decedent donors and then re-cellularized in vitro with autologous source of stem cells for soft tissue reconstruction.

Conclusion

Regardless of the protocols used for decellularization, the decellularized pieces of GOM preserved their shape, vascular architecture, and homogeneity with minimal deformation or disintegration. Although all the protocols showed the capability for a proper lipid removal and retention of neutral carbohydrate, collagen, and elastic fibers, SDS 1% (low concentration of SDS, hexane, acetone, EDTA, and ethanol) is considered the superior protocol for preservation of collagen and elastic fiber, protein, VEGF and GAGs.

Acknowledgments

The authors wish to thank the Research Deputy of Shiraz University of Medical Sciences for offering grant no 14418. This work was done by Kh.Fazelian-Dehkordi as a part of fulfillment for Ph.D. program. The authors would like to thank Shiraz University of Medical Sciences, Shiraz, Iran, and the Center for Development of Clinical Research of Nemazee Hospital and Dr. Nasrin Shokrpour for editorial assistance. The authors declare no conflict of interest.

Authors' Contributions

Kh.F.D.; Participated in all experimental work, data collection, evaluation, drafting, and statistical analysis. S.F.M.A.; Contributed to the study conception and design. T.T.-Kh.; Contributed extensively to the interpretation of the data, the conclusion, and revising of the draft. All authors read and approved the final manuscript.

References

1. Kim TH, Kim DY, Jung KH, Hong YS, Kim SY, Park JW, et al. The role of omental flap transposition in patients with locoregional recurrent rectal cancer treated with reirradiation. J Surg Oncol. 2010; 102(7): 789-795.
2. Di Nicola V. Omentum a powerful biological source in regenerative surgery. Regen Ther. 2019; 11: 182-191.
3. Porzionato A, Sfriso M, Macchi V, Rambaldo A, Lago G, Lancerotto L, et al. Decellularized omentum as novel biologic scaffold for reconstructive surgery and regenerative medicine. Eur J Histochem. 2013; 57(1): e4.
4. Soffer-Tsur N, Shevach M, Shapira A, Peer D, Dvir T. Optimizing the biofabrication process of omentum-based scaffolds for engineering autologous tissues. Biofabrication. 2014; 6(3): 035023.
5. Shevach M, Zax R, Abrahamov A, Fleischer S, Shapira A, Dvir T. Omentum ECM-based hydrogel as a platform for cardiac cell delivery. Biomed Mater. 2015; 10(3): 034106.
6. Baker NA, Muir LA, Washabaugh AR, Neeley CK, Chen SY-P, Flesher CG, et al. Diabetes-specific regulation of adipocyte metabolism by the adipose tissue extracellular matrix. J Clin Endocrinol Metab. 2017; 102(3): 1032-1043.
7. Lin T, Liu S, Chen S, Qiu S, Rao Z, Liu J, et al. Hydrogel derived from porcine decellularized nerve tissue as a promising biomaterial for repairing peripheral nerve defects. Acta Biomater. 2018; 73: 326-338.
8. Shevach M, Soffer-Tsur N, Fleischer S, Shapira A, Dvir T. Fabrication of omentum-based matrix for engineering vascularized cardiac tissues. Biofabrication. 2014; 6(2): 024101.
9. Loreto C, Leonardi R, Musumeci G, Pannone G, Castorina S. An ex vivo study on immunohistochemical localization of MMP-7 and MMP-9 in temporomandibular joint discs with internal derangement. Eur J Histochem. 2013; 57(2): e12.
10. Emami A, Talaei-Khozani T, Tavanafar S, Zareifard N, Azarpira N, Vojdani Z. Synergic effects of decellularized bone matrix, hydroxyapatite, and extracellular vesicles on repairing of the rabbit mandibular bone defect model. J Transl Med. 2020; 18(1): 1-18.
11. Porzionato A, Stocco E, Barbon S, Grandi F, Macchi V, De Caro R. Tissue-engineered grafts from human decellularized extracellular matrices: a systematic review and future perspectives. Int J Mol Sci. 2018; 19(12): 4117.
12. Crapo PM, Gilbert TW, Badylak SF. An overview of tissue and whole organ decellularization processes. Biomaterials. 2011; 32(12): 3233-3243.
13. Hoshiba T, Lu H, Kawazoe N, Chen G. Decellularized matrices for tissue engineering. Expert Opin Biol Ther. 2010; 10(12): 1717-1728.
14. Yang B, Zhang Y, Zhou L, Sun Z, Zheng J, Chen Y, et al. Development of a porcine bladder acellular matrix with well-preserved extracellular bioactive factors for tissue engineering. Tissue Eng Part C Methods. 2010; 16(5): 1201-1211.
15. Shupe T, Williams M, Brown A, Willenberg B, Petersen BE. Method for the decellularization of intact rat liver. Organogenesis. 2010; 6(2): 134-136.
16. Lumpkins SB, Pierre N, McFetridge PS. A mechanical evaluation of three decellularization methods in the design of a xenogeneic scaffold for tissue engineering the temporomandibular joint disc. Acta Biomater. 2008; 4(4): 808-816.
17. Hassanpour A, Talaei-Khozani T, Kargar-Abarghouei E, Razban V, Vojdani Z. Decellularized human ovarian scaffold based on a sodium lauryl ester sulfate (SLES)-treated protocol, as a natural three-dimensional scaffold for construction of bioengineered ovaries. Stem Cell Res Ther. 2018; 9(1): 252.
18. Geerts S, Ozer S, Jaramillo M, Yarmush ML, Uygun BE. Nondestructive methods for monitoring cell removal during rat liver decellularization. Tissue Eng Part C Methods. 2016; 22(7): 671-678.
19. Valipour Nouroozi R, Valipour Noroozi M, Ahmadizadeh M. Determination of protein concentration using bradford microplate protein quantification assay. Int Electron J Med. 2015; 4(1): 11-17.
20. Gilpin A, Yang Y. Decellularization strategies for regenerative medicine: from processing techniques to applications. Biomed Res Int. 2017; 2017: 9831534.
21. Talari ACS, Movasaghi Z, Rehman S, Rehman IU. Raman spectroscopy of biological tissues. Appl Spectrosc Rev. 2015; 50(1): 46-111.
22. Movasaghi Z, Rehman S, Rehman IU. Raman spectroscopy of biological tissues. Appl Spectrosc Rev. 2007; 42(5): 493-541.
23. Xing Q, Yates K, Tahtinen M, Shearier E, Qian Z, Zhao F. Decellularization of fibroblast cell sheets for natural extracellular matrix scaffold preparation. Tissue Eng Part C Methods. 2014; 21(1): 77-87.
24. Kargar-Abarghouei E, Vojdani Z, Hassanpour A, Alaee S, Talaei-Khozani T. Characterization, recellularization, and transplantation of rat decellularized testis scaffold with bone marrow-derived mesenchymal stem cells. Stem Cell Res Ther. 2018; 9(1): 1-16.
25. Ma J, Ju Z, Yu J, Qiao Y, Hou C, Wang C, et al. Decellularized rat

lung scaffolds using sodium lauryl ether sulfate for tissue engineering. Asaio J. 2018; 64(3): 406-414.
26. Naeem EM, Sajad D, Talaei-Khozani T, Khajeh S, Azarpira N, Alaei S, et al. Decellularized liver transplant could be recellularized in rat partial hepatectomy model. J Biomed Mater Res A. 2019; 107(11): 2576-2588.
27. Linhardt RJ, Toida T. Role of glycosaminoglycans in cellular communication. Acc Chem Res. 2004; 37(7): 431-438.
28. Ott HC, Clippinger B, Conrad C, Schuetz C, Pomerantseva I, Ikonomou L, et al. Regeneration and orthotopic transplantation of a bioartificial lung. Nat Med. 2010; 16(8): 927-933.
29. Reing JE, Brown BN, Daly KA, Freund JM, Gilbert TW, Hsiong SX, et al. The effects of processing methods upon mechanical and biologic properties of porcine dermal extracellular matrix scaffolds. Biomaterials. 2010; 31(33): 8626-8633.
30. Wang J, Jia R, Wang J, Sun Z, Wu Z, Liu R, et al. Investigation on the interaction of catalase with sodium lauryl sulfonate and the underlying mechanisms. J Biochem Mol Toxicol. 2018; 32(2): e22025.
31. Gholami M, Zare-Hoseinabadi A, Mohammadi M, Taghizadeh S, Behbahani AB, Amani AM, et al. Preparation of ZnXFe3-XO4@ chitosan nanoparticles as an adsorbent for methyl orange and phenol. J Environ Treat Tech. 2019; 7(3): 245-249.
32. Schwarz S, Koerber L, Elsaesser AF, Goldberg-Bockhorn E, Seitz AM, Dürselen L, et al. Decellularized cartilage matrix as a novel biomatrix for cartilage tissue-engineering applications. Tissue Eng Part A. 2012; 18(21-22): 2195-2209.
33. Schmitt A, Csiki R, Tron A, Saldamli B, Tübel J, Florian K, et al. Optimized protocol for whole organ decellularization. Eur J Med Res. 2017; 22(1): 1-9.
34. Omidi E, Fuetterer L, Mousavi SR, Armstrong RC, Flynn LE, Samani A. Characterization and assessment of hyperelastic and elastic properties of decellularized human adipose tissues. J Biomech. 2014; 47(15): 3657-3663.
35. Hassanpour A, Talaei-Khozani T, Kargar-Abarghouei E, Razban V, Vojdani Z. Decellularized human ovarian scaffold based on a sodium lauryl ester sulfate (SLES)-treated protocol, as a natural three-dimensional scaffold for construction of bioengineered ovaries. Stem Cell Res Ther. 2018; 9(1): 1-13.
36. Chung EJ, Ju HW, Yeon YK, Lee JS, Lee YJ, Seo YB, et al. Development of an omentum-cultured oesophageal scaffold reinforced by a 3D-printed ring: feasibility of an in vivo bioreactor. Artif Cells Nanomed Biotechnol. 2018; 46 Suppl1: 885-895.
37. Buyukdogan K, Doral MN, Bilge O, Turhan E, Huri G, Sargon MF. Peritoneum and omentum are natural reservoirs for chondrocytes of osteochondral autografts: a comparative animal study. Acta Orthop Traumatol Turc. 2016; 50(5): 539-543.
38. Collins D, Hogan AM, O'Shea D, Winter DC. The omentum: anatomical, metabolic, and surgical aspects. J Gastrointest Surg. 2009; 13(6): 1138-1146.
39. Kant RJ, Coulombe KL. Integrated approaches to spatiotemporally directing angiogenesis in host and engineered tissues. Acta Biomater. 2018; 69: 42-62.